A MORPHOMETRICAL STUDY OF THE EXOCRINE PANCREATIC CELL IN FASTED AND FED FROGS

J. W. SLOT and J. J. GEUZE

From the Center for Electron Microscopy, University of Utrecht Medical School, Utrecht, The Netherlands

ABSTRACT

The influence of feeding on the ultrastructure of the frog exocrine pancreatic cell was studied by morphometrical procedures. Volume and surface of various cell structures were measured and expressed per unit cell volume. The average cellular size was not influenced by feeding. Though protein synthesis changes 5- to 10-fold (van Venrooij, W. J., and C. Poort. 1971. *Biochim. Biophys. Acta.* **247**:468–470), no significant differences were observed in the amount of membrane that constitutes the rough endoplasmic reticulum (RER) and that represented the major part of total cellular membranes. The appearance of the RER changed. When fasted, most of its membrane was arranged in stacks of tightly packed, narrow cisternae. Within 4 h after feeding, these cisternae were separated and irregularly dilated, and ribosomes became ordered in typical rosettes on their surface.

The total volume of the Golgi system increased twofold after feeding. The vesicular and tubular elements at the Golgi periphery did not change, but the volumes of the Golgi cisternae and the condensing vacuoles increased 2.5- and 6-fold, respectively. The increase in the amount of membrane present in these structures was only 1.6- and 3.5-fold, which reflects the more distended appearance of the cisternae and the rounded shape of the condensing vacuoles after feeding. Feeding halved the number of secretory granules per cell, and signs of exocytosis were more common than in fasted animals.

These findings suggest that, in the frog pancreatic cell, fluctuations in the production of secretory proteins are not accompanied by an important breakdown and renewal of cellular membranes. This may favor a rapid and strong response of the cell to feeding.

KEY WORDS frog · exocrine pancreas · feeding · ultrastructure · morphometry

The exocrine pancreas is a typical serous gland, composed of cells with a regular structural polarity, which makes the pancreas a favorable tissue for studies on synthesis, intracellular transport, release of secretory proteins (14, 15, 18, 29, 32), and on related membrane regulation (9, 10, 13, 21, 22). Most work has been done on mammalian tissue, in which the rate of protein synthesis is not influenced or is only slightly influenced by feeding or secretory stimuli (15, 18, 24, 31). In the pancreas of the frog, however, the rate of protein synthesis is closely dependent on the feeding condition. Previously, our group demonstrated

J. CELL BIOLOGY © The Rockefeller University Press · 0021-9525/79/03/0692-16$1.00
Volume 80 March 1979 692–707

that protein synthesis rises 5- to 10-fold within 4 h after feeding and decreases again to a basal level within 10 h (38).

We studied the effects of the feeding stimulus on the function and structure of the exocrine pancreatic cells of the frog. The present paper gives a morphometric analysis of the cells in fasted and fed conditions. The companion article deals with the influence of fasting and feeding on synthesis and intracellular transport of proteins in these cells (36).

MATERIALS AND METHODS

Animals

Frogs (*Rana esculenta*), which weighed 20–40 g, were kept at 22°C in a tank with a sloping bottom, which was partly covered by tap water. They were force-fed with 100 mg of meat two or three times a week. Alternate periods of 12-h light and 12-h darkness were kept in phase with the actual day-night rhythm. The animals were killed by decapitation 4 h (fed animals) or 48 h (fasted animals) after feeding, unless indicated otherwise.

Tissue Processing

Pieces of pancreas were put into a drop of fixation fluid on the table of a TC-2 Sorvall tissue sectioner (DuPont Instruments-Sorvall, DuPont Co., Newtown, Conn.) and chopped in two perpendicular directions (stroke distance, 0.5 mm). Subsequently, the tissue was processed as previously described (34). Briefly, fragments were fixed in 1% OsO_4 in 0.07 M Veronal buffer (pH 7.4) for 2 h, stained in uranyl acetate, and embedded in Epon 812. Greyish sections were stained with lead citrate. Micrographs were taken with a Siemens Elmiskop I or Philips EM 301 electron microscope.

Some tissue fragments were impregnated with osmium by treatment with unbuffered 2% OsO_4 at 37°C for 40 h (7). Further processing was the same as that for normally fixed tissue. Osmium-impregnated tissue was studied under the electron microscope in semi-thin (200 nm) or thin (greyish) sections.

Morphometry

SAMPLING: From each of five fasted and five fed animals, two tissue blocks were randomly taken out of a stock of 20. By operating at low magnification and using greyish sections, we selected areas at a distance of at least 50 μm from the cutting edges of the blocks. Series of micrographs were taken by a systematic sampling procedure. Magnification varied with the dimensions of the structures to be measured (see below) and were calibrated with the aid of a replica grid (2,160 lines/mm). To estimate how many micrographs were needed to obtain a representative sample, we employed the method of "progressive calculation of the means" (4). By pooling increasing numbers of micrographs, the sample size that was finally used showed variations of the volumetric means of 10% for all cell structures measured.

The micrographs were analyzed with the aid of a transparent screen marked with a squared lattice of lines. The intersections of the lines served as test points. The number and spacing of the lines were determined by the method of Weibel and Bolender (40). For all cell structures that were quantitated, except lipid droplets and lysosomes, the test-point density (1 point/cm^2) exceeded the number giving relative errors of 5%. The following morphometrical parameters were determined:

Volume density (Vv_i^{ex}), the volume of a component i per unit volume exocrine cell (ex). 20–24 micrographs with a final magnification of × 12,000 were used per animal. Test points were counted over RER, Golgi system, secretory granules, cell membrane, lysosomes, lipid droplets, mitochondria, and nucleus. Points over the cytoplasmic matrix were attributed to the nearest of the following structures: RER, Golgi system, and cell membrane. The necessity to do so is amplified in the results. The item cell membrane includes small vesicles that were often observed near the cell membrane. Volume density was calculated from:

$$Vv_i^{ex} = \frac{\text{test points over } i}{\text{total test points over exocrine cells}}.$$

Surface-to-volume ratio (S/V_i), the surface area of a structure i per unit volume occupied by that structure. This was established for RER, secretory granules, and cell membrane from 16 micrographs per animal, with a final magnification of × 30,000. The number of test points over these structures and the number of intersections of their limiting membrane with a superimposed line probe (1 cm/cm^2) were counted. Then the surface-to-volume ratio was calculated from:

$$S/V_i = 2 \times \frac{\text{number intersections with } i}{\text{test points over } i} \times \text{magnification}.$$

The values calculated in this way were divided by 10^4 so that the data are expressed as $\mu m^2/\mu m^3$ (Table III).

Substructures of the Golgi system were measured in section areas comprising one or two grid meshes (0.04 mm^2) which were selected at low magnification. All Golgi profiles in their areas were photographed and printed at a final magnification of × 30,000. The Vv_i^{ex} of the following Golgi substructures was measured by the "multiple stage" procedure (3): (*a*) Golgi periphery, which is the cytoplasmic area with vesicular and tubular structures (the peripheral elements) at the outer (convex) side of Golgi system facing the RER; (*b*) Golgi cisternae; (*c*) condensing vacuoles; and (*d*) Golgi center, the cytoplasmic area at the inner (concave) side of the stacks of cisternae that fills up the space between the

condensing vacuoles. The cytoplasmic matrix within the Golgi system was added to substructures (*a*) or (*d*). Determination of volume and surface values of the small membranous structures in substructures (*a*) and (*d*) appeared too complicated because these structures had very irregular shapes and, at least in one dimension, their size was less than the section thickness. The test point system (1 point/cm^2) was used to establish the relative volume of the Golgi substructures within the Golgi system (Vv_i^{gs}). To get Vv_i^{ex} for these substructures, Vv_i^{gs} was multiplied by Vv_{gs}^{ex}. S/V_i for Golgi cisternae and condensing vacuoles was established from the same micrographs.

Surface density (Sv_i^{ex}), the surface area of a structure i per unit volume exocrine cell was calculated from:

$$Sv_i^{ex} = Vv_i^{ex} \times S/V_i.$$

Nuclear size. The average nuclear size was estimated from micrographs with a magnification of × 2,400. By counting the number of points of a test point system (25 points/cm^2) over nuclear profiles, the area of each profile was measured and the mean diameter was calculated as if they were circular. The diameters of 500 nuclear profiles in both fasted and fed animals were grouped into 13 size classes. From the histogram formed by these size classes, the mean nuclear diameter was determined by the method of Giger and Riedwyl (11, see also reference 40). From the mean nuclear diameter, the mean nuclear volume was calculated which was divided by Vv_n^{ex} to give the mean cell volume.

Section compression during cutting was measured by determining the ratio of two diameters, one perpendicular and one parallel to the cutting direction, of 15 secretory granule profiles in each specimen used. Secretory granules were assumed to be normally globular. Compression was almost similar in tissue from fasted and fed animals: the mean ratios were 0.803 ± 0.013 and 0.796 ± 0.007 (± SEM), respectively.

RESULTS

In previous work we showed that the ultrastructure of the exocrine pancreatic cell of the frog was essentially identical to that in mammals (34). Here we report morphological changes in the frog exocrine pancreatic cell that accompany feeding stimuli after physiological periods of fasting. To this end, the structures of these cells in fasted (48 h after feeding) and fed (4 h after feeding) animals were compared both qualitatively and quantitatively. We worked with 4-h fed animals on the basis of previous work, which showed that feeding induces a strong increase of protein synthesis that is maximal after 4 h. 10 h after feeding, protein synthesis is again at a low level (38), which remains constant for several days (unpublished observations). Hence, the choice of 48 h guaranteed tissue with a basal, low state of activity with respect to zymogen production.

The general appearance of the cells, after both fasting and feeding, is shown in Figs. 1 and 2. All quantitative data gained by morphometry are summarized in Tables I, II, and III. Volume density (Vv_i^{ex}) values are given in Tables I and II. Surface to volume ratio (S/V_i) and surface density (Sv_i^{ex}) are tabulated in Table III.

The Nucleus

The nucleus was roughly spherical in both fasted and fed animals, but after fasting its outline was more irregular. The mean nuclear diameter (± SD) as measured by the Giger-Riedwyl procedure was 7.28 ± 0.77 μm in fasted and 7.87 ± 0.75 μm in fed animals.[1] These diameters correspond to mean nuclear volumes of 209 and 262 μm^3, respectively. Thus, the nuclear volume increased by 25% after feeding. Vv_n^{ex} increased proportionally. The mean cellular volume, calculated as the ratio of the mean nuclear volume and Vv_n^{ex} is 1,490 μm^3 after fasting and 1,507 μm^3 after feeding. Thus, feeding does not cause an important change in cell volume. This implies that the morphometrical data expressed per cubic millimeter exocrine cell (Tables I, II, and III) can be considered as reflecting the situation per cell.

The less undulating boundary after feeding suggests a smaller surface-to-volume ratio of the nucleus. From fasted and fed animals, 10 approxi-

[1] A troublesome point in our measurements was that the nuclei, after fasting, had irregular contours for which no correction could be made. The following considerations show that this, at worst, introduced only a minor error in our calculations: (*a*) The undulating nuclear surface after fasting resulted mainly in overrating the number of very small profiles. The Giger-Riedwyl procedure includes a correction for an error normally made in this small category. Therefore, the error made by overrating the small profiles will not influence the calculation. (*b*) The shapes of the corrected histograms in which the nuclear profiles were plotted by their diameter were not very different for the fasted and fed animals, as is illustrated by the almost equal standard deviations. This indicates that the three-dimensional shapes from which the nuclear profiles were derived are not very different. (*c*) The direct comparison of the nuclear shape in series of 10 nuclear profiles in fasted and fed conditions was in agreement with a nuclear growth by 25%. (*d*) The finding that the cell volume does not change is in good accordance with the fact that the volume density of mitochondria, which are not directly involved in the processing of secretory proteins, remained unchanged.

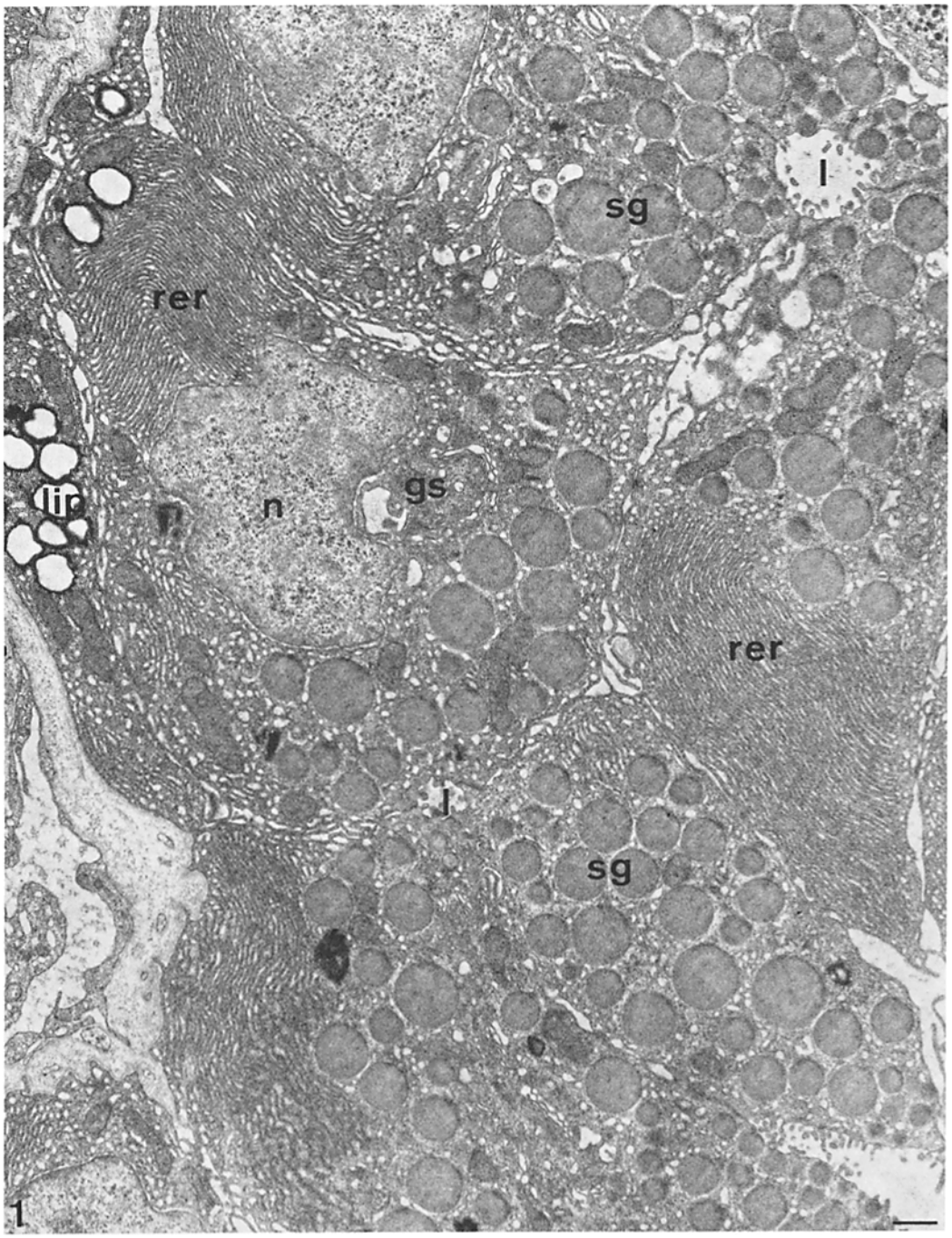

FIGURE 1 Exocrine pancreatic tissue of a fasted frog. Fingerprint-like figures of tightly packed RER cisternae occur in the basal part of the cells (*rer*), where lipid droplets (*lip*) are occasionally also present. Vesicular RER is found in the middle and apical regions of the cells. The nucleus (*n*) has an undulating outline. The Golgi system (*gs*) is a rather compact structure. The apices of the cells contain numerous secretory granules (*sg*) and bear many microvilli protruding into the secretory lumen (*l*). Bar, 1 μm. × 7,200.

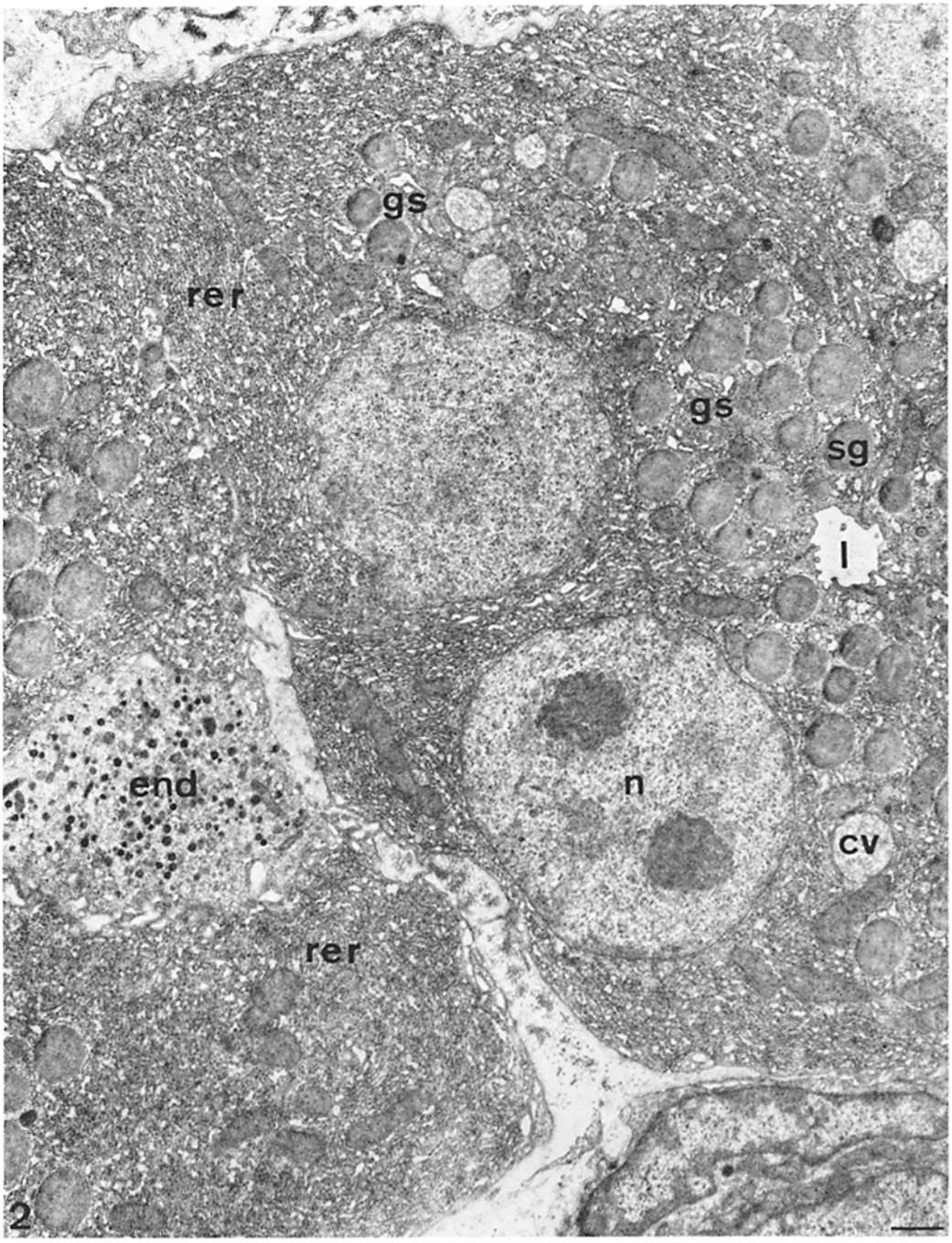

FIGURE 2 Exocrine- and endocrine (*end*)-pancreatic tissue of a fed frog. The RER is uniformly constituted of rather irregular cisternae. The nucleus has an almost spherical shape. The Golgi system is extended and contains many condensing vacuoles (*cv*). Only a few, relatively short microvilli are visible at the luminal cell membrane. Abbreviations are as in Fig. 1. Bar, 1 μm. × 7,200.

TABLE I

Volume Density (Vv_i^{ex}) and SEM of Cell Structures in Frog Exocrine Pancreatic Cells 48 h (Fasted) and 4 h (Fed) after Feeding

	Fasted	Fed	P‡
RER (*rer*)*	0.5990 ± 0.0104	0.6014 ± 0.0085	NS
Golgi system (*gs*)	0.0282 ± 0.0016	0.0648 ± 0.0051	<0.001
Secretory granules (*sg*)	0.1266 ± 0.0097	0.0638 ± 0.0070	<0.001
Cell membrane	0.0544 ± 0.0026	0.0492 ± 0.0081	NS
Lysosomes (*ly*)	0.0060 ± 0.0009	0.0020 ± 0.0003	<0.005
Lipid droplets	0.0016 ± 0.0009	0.0006 ± 0.0003	NS
Mitochondria	0.0488 ± 0.0021	0.0478 ± 0.0027	NS
Nucleus (*n*)	0.1356 ± 0.0085	0.1692 ± 0.0079	<0.01

* The abbreviations indicated here and in Table II are used for the stereological notation in the text.

‡ *P* values here and in Tables II and III show the level of significance for differences between data from fasted and fed animals. No significance (NS) was attributed to $P > 0.1$.

TABLE II

Volume Density and SEM of Golgi Substructures in Frog Exocrine Pancreatic Cells Expressed Per Unit Volume Golgi System (Vv_i^{gs}) and Per Unit Volume Exocrine Cell (Vv_i^{ex}), 48 h (Fasted) and 4 h (Fed) after Feeding

	Vv_i^{gs}			Vv_i^{ex}		
	Fasted	Fed	*P*	Fasted	Fed	*P*
Periphery (*gpe*)	0.2764 ± 0.0139	0.1528 ± 0.0029	<0.001	0.0079 ± 0.0006	0.0099 ± 0.0008	<0.05
Cisternaf (*gci*)	0.2864 ± 0.0098	0.3180 ± 0.0126	<0.05	0.0082 ± 0.0005	0.0206 ± 0.0018	<0.001
Condensing vacuoles (*cv*)	0.1248 ± 0.0141	0.3292 ± 0.0169	<0.001	0.0036 ± 0.0004	0.0213 ± 0.0020	<0.001
Center (*gce*)	0.3120 ± 0.0094	0.1998 ± 0.0051	<0.001	0.0084 ± 0.0005	0.0129 ± 0.0011	<0.005

TABLE III

Surface-to-Volume Ratio (S/V_i) and Surface Density per Unit Volume Exocrine Cell (Sv_i^{ex}) of Cell Structures in the Frog Pancreas ($\mu m^2/\mu m^3$ ± SEM)

	S/V_i			Sv_i^{ex}		
	Fasted	Fed	*P*	Fasted	Fed	*P*
RER	15.26 ± 0.52	14.92 ± 0.37	NS	9.141 ± 0.348	8.970 ± 0.258	NS
Golgi cisternae	24.16 ± 0.97	15.22 ± 0.92	<0.001	0.195 ± 0.014	0.314 ± 0.031	<0.005
Condensing vacuoles	8.88 ± 0.79	5.42 ± 0.46	<0.005	0.031 ± 0.003	0.116 ± 0.013	<0.001
Secretory granules	4.80 ± 0.41	4.90 ± 0.13	NS	0.608 ± 0.069	0.312 ± 0.035	<0.005
Cell membrane	21.22 ± 1.15	22.01 ± 1.43	NS	1.154 ± 0.096	1.082 ± 0.191	NS

mately equatorial nuclear profiles were photographed and printed at × 6,300. Nuclear surfaces and perimeters were measured with the aid of a planimeter and a curvimeter, respectively. The average surface of these profiles corresponded to that of a circle with a Diam of 7.55 μm after fasting and 8.27 μm after feeding. The average perimeter of the same profiles equaled that of a circle with a Diam of 8.44 μm after fasting and 8.27 μm after feeding. This indicates that the increase in the nuclear volume was not accompanied by a growth of the nuclear envelope, but only by a smoothening of its wrinkled surface.

The RER

After fasting, two types of RER could be discerned. The first (Fig. 3) was present in the basal part of the cells and was composed of stacks of strictly parallel lamellae, appearing as fingerprint-like figures in cross sections. The ribosomes were randomly distributed over the surface of the lamellae (see *inset* Fig. 3). Interconnections between the lamellae were not observed, and fenestrae as described in pancreatic tissue by Orci et al. (27) were seen only in the outermost lamellae. The second type of RER was composed of micro-

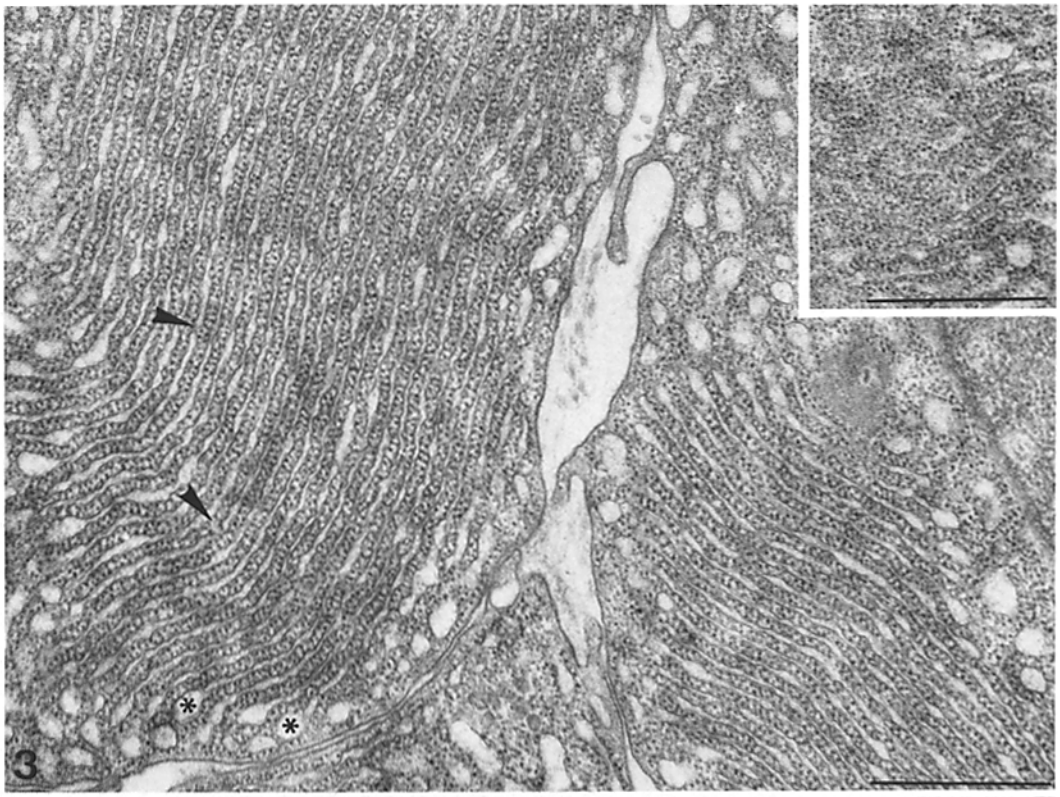
3

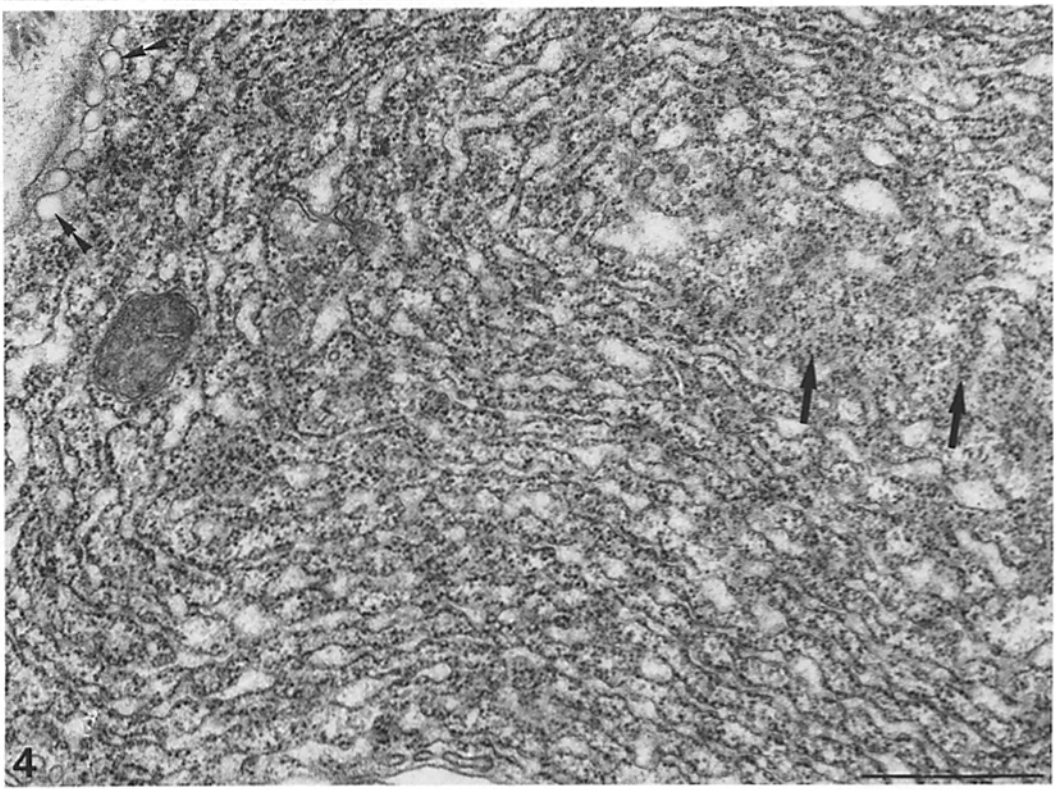
4

some-like vesicles. This type was especially prominent in the apical part of the cells between the secretory granules and surrounding the Golgi system. Between these RER vesicles, many free ribosomes occurred.

In the fed animal the main part of the RER was of the lamellar type, but the inter- as well as intralamellar spaces were more irregular and wider than in the lamellar RER described in fasted animals (Fig. 4). Fenestrae and interconnections were rare, but they might have been overlooked because of the undulating course of the RER membranes. The membranes were covered by ribosomes, often arranged in rosettes, most probably reflecting the polysomes demonstrated earlier in this tissue after feeding (38).

Accurate measurement of the stereological parameters of the RER per se was impossible because the RER membranes were often cut obliquely or tangentially, which hampered the decision as to whether probe points fell over the RER or over the narrow strands of cytoplasm intervening the RER in the volume measurements. Hence, the Vv^{ex}_{rer} refers to the volume of the cellular region occupied by the RER. In both the fasted and fed conditions, Vv^{ex}_{rer} was about the same (Table I). Together with the adjoining strands of cytoplasmic matrix, the RER occupied 60% of the cell volume. We further measured the RER surface values and related them to the volume values. In contrast with the points, the intersection of the probe lines with the RER membranes could be established and their number could be counted even in the case of oblique membrane aspects. The combined interpretation of Vv^{ex}_{rer} and S/V_{rer} reveals that the volume of the RER, including the accompanying part of the cytoplasmic matrix, and the amount of RER membrane are similar in both feeding conditions. Apparently, the high surface-to-volume ratio of the lamellar RER after fasting is compensated by a low value for the vesicular type.

The Golgi System

The Golgi system was well demarcated in osmium-impregnated tissue (Figs. 5 and 6). This technique selectively stains the side of the Golgi system facing the RER (34). In fasted animals, the Golgi system was roughly globular and often located between the secretory granules. The stained Golgi elements formed a more or less closed ring (Fig. 5). After feeding, the osmicated Golgi elements were dispersed throughout the cell apex, showing that the organelle had lost its globular shape (Fig. 6). At higher magnification, some differences could be observed in the appearance of the stained parts themselves. After fasting, osmium deposits were especially observed in peripheral vesicles and tubules (Fig. 7). Buds at the transitional elements of the RER were never blackened by osmium (Fig. 8). After feeding, extended and intensively staining tubular meshworks had been formed, constituting the outermost Golgi cisternae (Fig. 9). A relatively smaller part of the osmium deposits was found in the peripheral elements.

Observations of the Golgi system in normally fixed tissue confirmed that, after fasting, the peripheral elements were very prominent (Fig. 10). The dilated Golgi cisternae looked empty. The innermost cisternae were slender and often reminiscent of flattened lamellae in the Golgi center. These lamellae were of the type recently described as GERL-like structures in serous cells (12, 26). Condensing vacuoles were scarce, had an irregular shape, contained little electron-dense content, and were often connected to the lamellae (Figs. 10 and 11). Complexes of condensing vacuoles and lamellae were sometimes seen (Fig. 12). In addition to the lamellae, the Golgi center contained

FIGURE 3 Basal parts of exocrine cells after fasting show stacks of typical lamellar RER. The distance between the lamellae is constant. The width of the intracisternal space is more variable and often distended at the ends of the lamellae (asterisks). Fenestrae in the piled RER cisternae are scarce (arrowheads). *Inset*: A tangential view of the RER cisternae, showing a random distribution of the membrane-attached ribosomes. Both bars, 1 μm. × 25,000.

FIGURE 4 Typical RER aspect after feeding. The cisternae are relatively distended here, and there is more space between them, but both intra- and inter-cisternal spaces vary considerably. In a tangential view of the membranes it can be seen that ribosomes are arranged in polysomelike figures (arrows). Smooth vesicles can be seen near the basal and lateral cell membrane (double arrowheads). Bar, 1 μm. × 25,000.

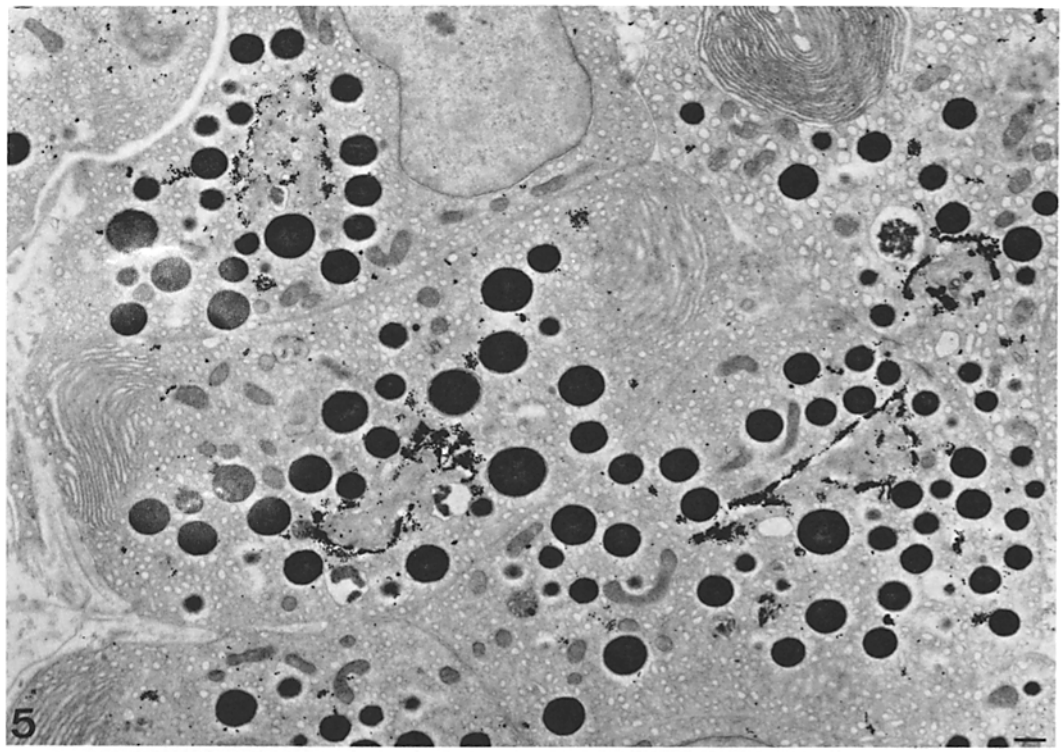

5

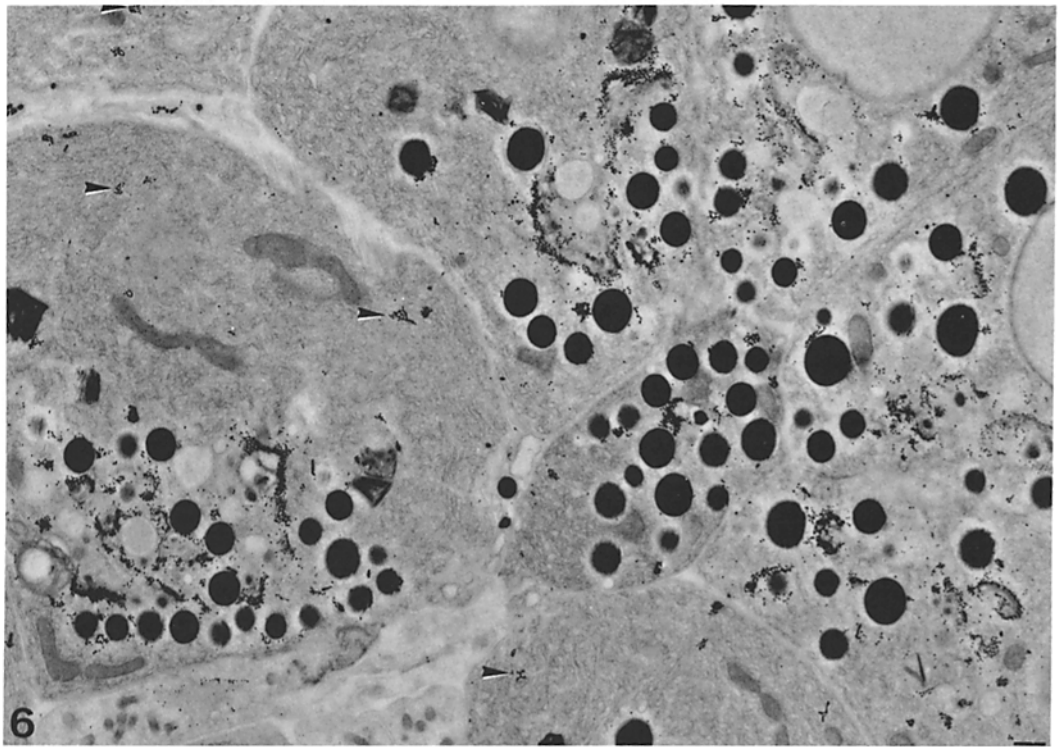

6

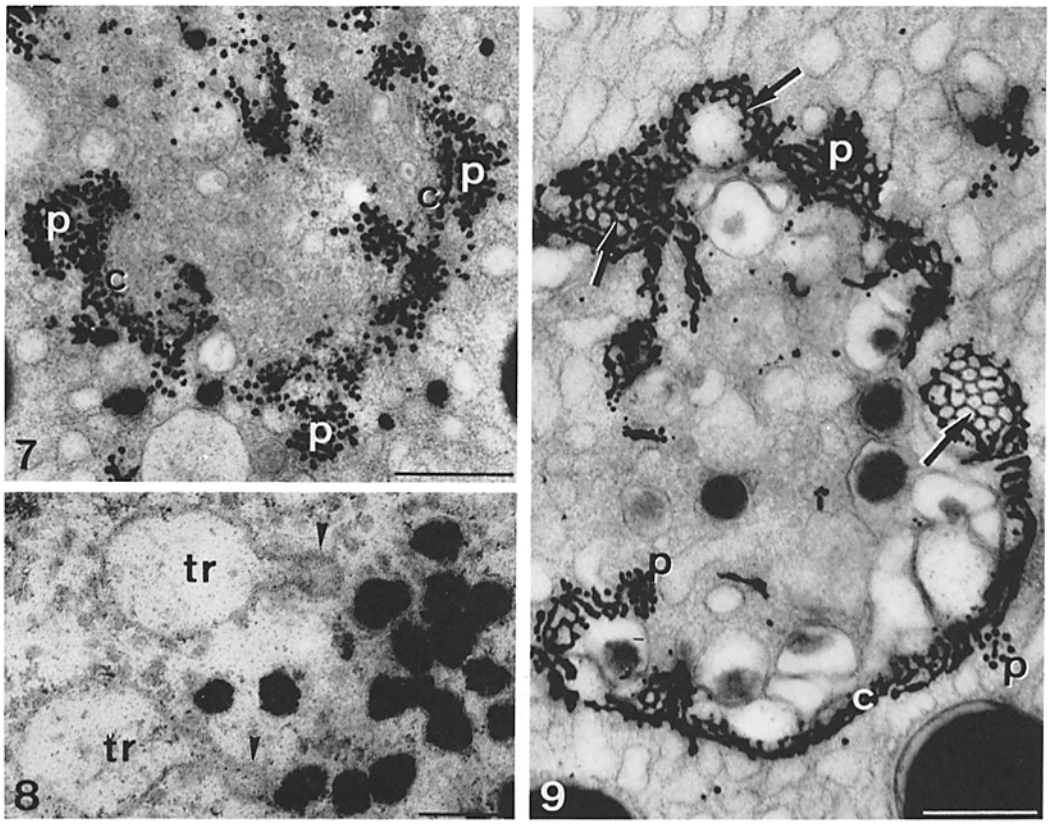

FIGURES 5–9 Semi-thin (~200 nm, Figs. 5–7, 9) and thin (~50 mm, Fig. 8) sections of osmium-impregnated pancreatic tissue.

FIGURE 5 Fasted frog. Stained elements mark clearly the outline of the Golgi system, which is a rather globular structure between the secretory granules. Bar, 1 μm. × 4,200.

FIGURE 6 Fed frog. Stained Golgi elements are scattered throughout the cell apices. Note that small clusters of stained tubules occur between the RER cisternae (arrowheads). Bar, 1 μm. × 4,200.

FIGURE 7 Golgi system after fasting. Osmium black is mainly present in the peripheral elements (*p*) and to a much lesser extent in the cisternae (*c*). 200-nm section. Bar, 1 μm. × 16,000.

FIGURE 8 Peripheral region of a Golgi system after fasting. Stained peripheral elements are in the immediate vicinity of unstained, stalked buds (arrowheads) on the transitional elements of the RER (*tr*). Bar, 0.1 μm. × 110,000.

FIGURE 9 Golgi system after feeding. The outermost Golgi cisternae (*c*) are remarkably elaborate and contain most of the osmium deposit. In tangential view it can be seen that the cisternae are composed of anastomosing tubules, which lie as a meshwork over the dilated, unstained inner cisternae (arrow). Clusters of peripheral elements (*p*) are also stained, but these are less predominant than after fasting. Bar, 1 μm. × 15,000.

numerous small vesicles and tubules. Many of the largest vesicles were coated, as were large parts of the condensing vacuole membranes.

After feeding, the peripheral elements were less conspicuous, formed small clusters, and contained more tubular structures than after fasting. These tubules were often continuous with the outermost Golgi cisternae. The Golgi cisternae had constricted and dilated portions. The latter often contained varying amounts of flocculent material (Fig. 13). Condensing vacuoles were numerous, spherical, and filled with flocculent material. Be-

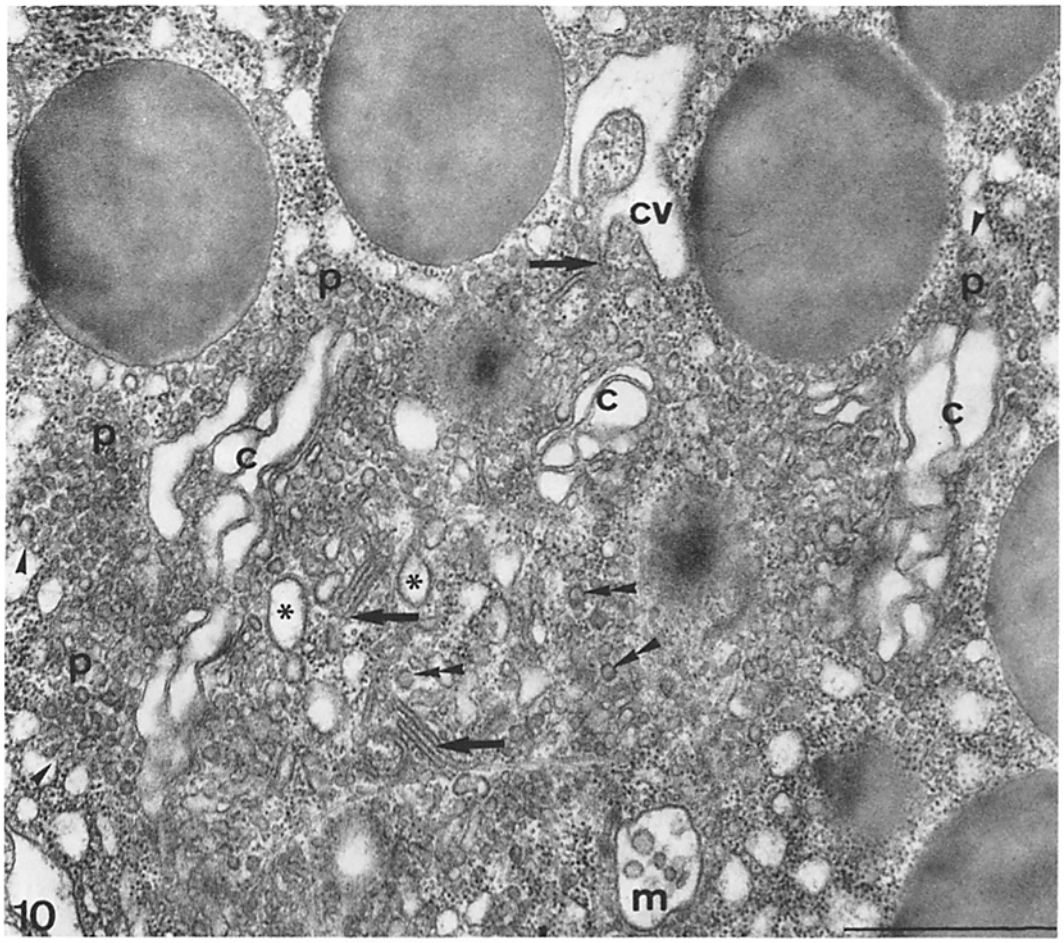
cv
p
p
p
p
c
c
c
*
*
m
10

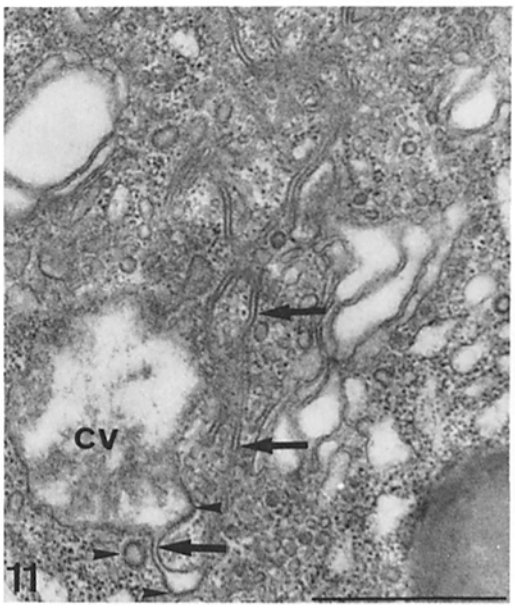
cv
11

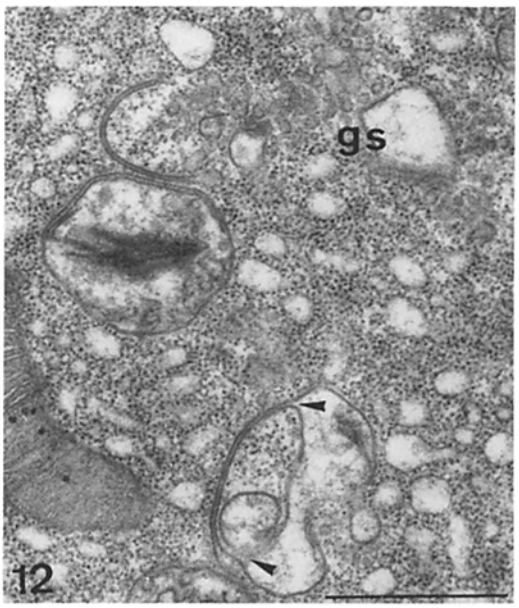
gs
12

cause the Golgi system was dispersed, the Golgi center was a less demarcated area than after fasting, but it was still recognizable by the presence of the characteristic vesicles, tubules, and lamellae.

Morphometry showed that, after feeding, the volume of the Golgi system increased twofold. The doubling of Vv_{gs}^{ex} was mainly caused by the increase of Vv_{gci}^{ex} (2.5 ×) and Vv_{cv}^{ex} (6.0 ×). S/V_{gci} and S/V_{cv} decreased strongly, reflecting the more distended appearance of the cisternae and the larger sizes and more spherical shape of the condensing vacuoles. Vv_{gpe}^{ex} and Vv_{gce}^{ex} increased only slightly.

The Secretory Granules

The secretory granules were less numerous after feeding. Vv_{sg}^{ex} had decreased to 50%. The granule profiles were approximately spherical. For spherical corpuscles, $S/V = 4\pi r^2/\frac{4}{3}\pi r^3 = 3/r$, or: r (radius) = $3/(S/V)$. Thus, we estimated from the S/V_{sg} a mean radius of 0.61 μm after fasting and 0.62 μm after feeding. Therefore, granule size does not increase after feeding as was reported for the parotid gland of rabbits (2). From the values reported for the pancreatic secretory granules in the guinea pig (3), a radius of 0.62 μm can be deduced. Thus the granules in frog and guinea pig have similar sizes.

Other Structures

The apical cell surface in fasted animals showed many microvilli (Fig. 1). When the animals were fed, microvilli were relatively sparse (Fig. 2) and the outline of the lumina was often very irregular, probably caused by exocytosis of secretory granules (Fig. 14). Small vesicles were often observed near the lateral and basal cell membranes (Fig. 4). For morphometry, these were grouped together with the cell membrane. The total amount of cell membrane thus measured showed no conspicuous differences after feeding.

After fasting, lysosomes occurred frequently in the vicinity of the Golgi system and between the basal RER lamellae. After feeding, Vv_{ly}^{cx} decreased significantly. Groups of lipid droplets occurred occasionally in the basal part of cells.

In addition to the observations at 4 and 48 h, tissue was studied from animals killed at 2, 6, 8, and 24 h, and 7 d after they were fed. At 24 h and 7 d the tissue looked similar to that at 48 h. From 2 to 8 h, the ultrastructure differed only slightly from that in the fed animals described above. Lipid droplets surrounded by mitochondria were sometimes observed at 2 h (Fig. 15). Signs of exocytosis were present from 2 to 6 h after feeding. At none of the time intervals was extensive autolytic degradation of the main cell structures encountered.

DISCUSSION

We used stereological procedures to study the ultrastructure of exocrine pancreatic cells with a low and high state of activity. However, the appearance of the tissue components in the thin sections was not always suitable to meet mathematical standards completely. For instance, the volume density of the cytoplasmic matrix (ground substance) could not be established, because of the small and irregularly shaped peripheral and central Golgi substructures and because of the numerous oblique and tangential aspects of the RER cisternae and cell membranes in the sections. Therefore, the cytoplasmic matrix was clas-

FIGURE 10 Golgi system of an exocrine pancreatic cell in the fasted frog. Large areas with peripheral elements (*p*) occur, accompanied by buds at the transitional elements of the RER (arrowheads). Empty, moderately dilated cisternae (*c*) border the central area. This area contains lamellar structures (arrows) and many vesicles, some of which are coated (double arrowheads). Some relatively small condensing vacuoles have coated limiting membranes as well (asterisks). Note the large, irregular condensing vacuole (*cv*) which is continuous with a lamellar structure. (*m*), Multivesicular body. Bar, 1 μm. × 30,000.

FIGURE 11 Fasted animal. A large condensing vacuole (*cv*) is connected to a lamellar structure (arrows). At some sites, the limiting membrane of this complex shows the same coating (arrowheads) as that seen on the coated vesicles. Bar, 1 μm. × 26,000.

FIGURE 12 Fasted animal. Lamellar structures in the vicinity of the Golgi system (*gs*). Some of them are connected in a remarkable way (arrowheads) to structures which probably represent condensing vacuoles. Bar, 1 μm. × 25,000.

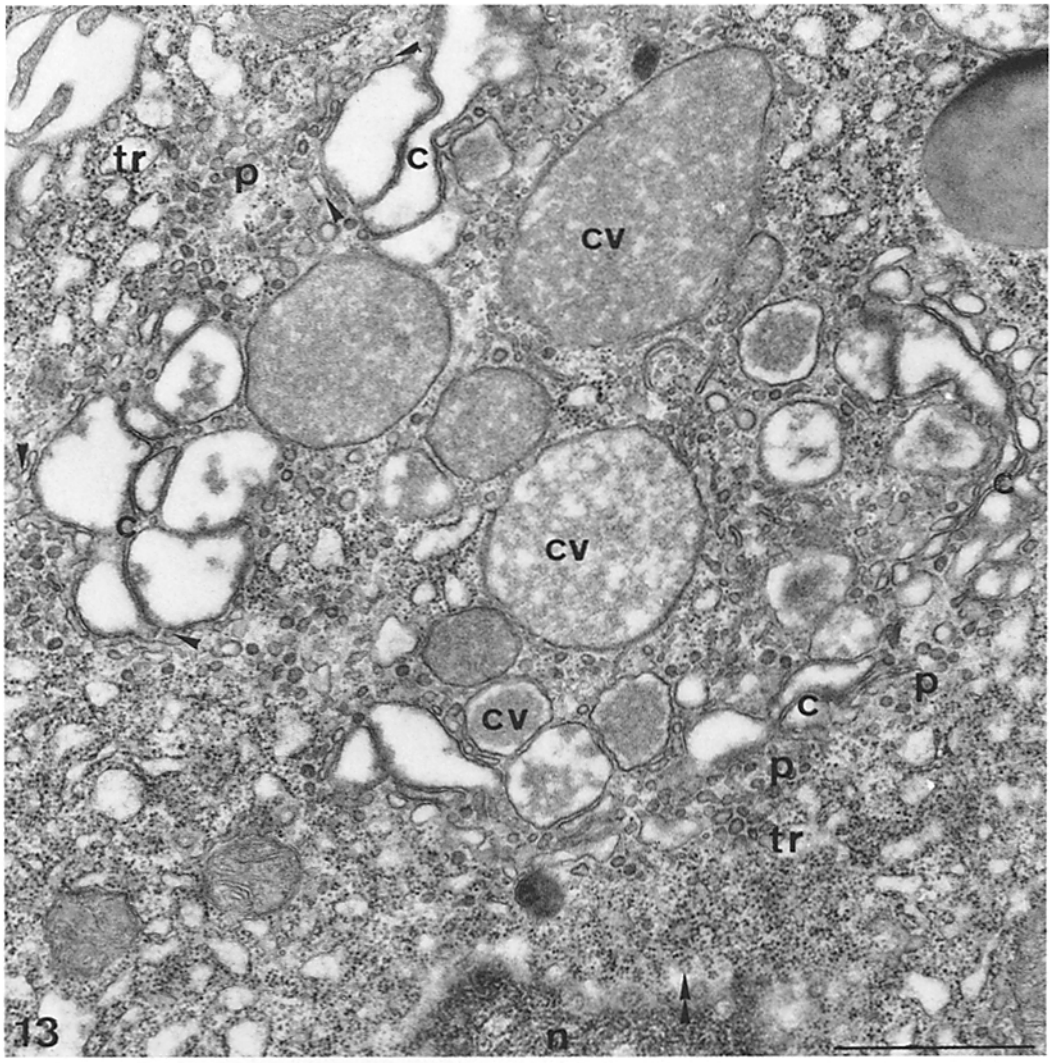
tr
p
c
cv
c
cv
c
p
cv
c
p
tr
13
n

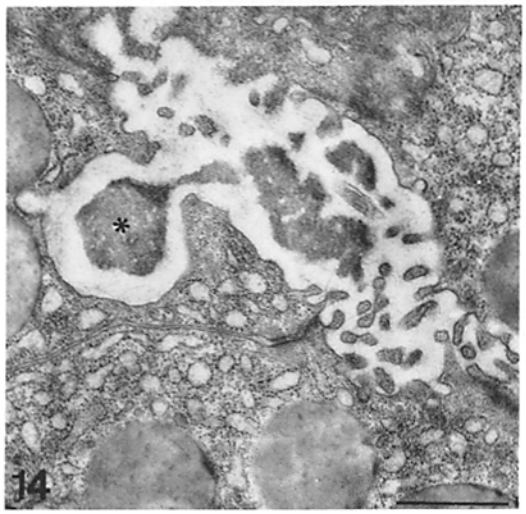
*
14

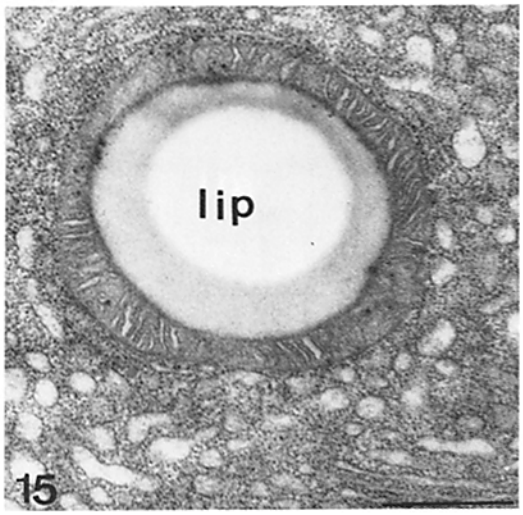
lip
15

sified within these items. Comparison of our data with those of Bolender (3) shows that the mean volume of the frog pancreatic cell is ~50% and that its nucleus (after feeding) is ~150% larger than in the guinea pig. Possibly, a relatively large nucleus is characteristic for frogs, because the DNA content per cell in these animals is twice that of mammals (37). In both species, volume density values for the other cell structures and the contribution of their membranes to the cellular membrane pool seem rather similar.

The RER is the predominant structure in the cytoplasm, containing ~80% of the cellular membranes (mitochondria excluded). In the frog, volume values and surface-to-volume ratio of the RER are about the same after fasting and feeding, although the rate of protein synthesis differs 5- to 10-fold. In other secretory cell types, a different situation has been described (5, 8, 17, 28, 30, 33), showing a close relationship between the development of the RER and the rate of protein synthesis. Mouse pancreas, in contrast to pancreas in other mammals (24, 31), shows a conspicuous decrease of protein synthesis after fasting (6). This is accompanied by extensive degenerative changes in the cells together with the formation of fingerprint-like RER figures (25). In the fasted frog, where protein synthesis is also very low, we observed a similar RER configuration but no signs of lytic breakdown of the RER. Apparently, the fingerprint-like structures represent a resting state of the RER, from which the active configuration is quickly restored after feeding.

At the periphery of the Golgi system, small vesicles are thought to carry the proteins from the RER to the Golgi cisternae, meanwhile fusing to form tubules (34, 35). The vesicles most likely arise from transitional elements of the RER. The concept of protein transport from the RER to the Golgi system via vesicles implies that large amounts of membrane are added to the Golgi system. During the repackaging of the secretory product from small peripheral Golgi vesicles into large secretory granules, the surface-to-volume ratio obviously decreases considerably. For spherical structures, this ratio is 3/r. Both the peripheral vesicles and the secretory granules are nearly spherical, so that a certain volume needs 20-fold more limiting membrane in the vesicles (r = 0.03 μm) than in the granules (r = 0.6 μm). Moreover, pancreatic secretory proteins are concentrated at least fivefold (1) during their transport through the cell. Hence, secretory products are packed (20 × 5 =) 100-fold more efficiently in the secretory granules than at the moment they enter the Golgi system. This means that for the final packaging of the secretory proteins an amount of membrane is needed that equals only 1% of the membrane supplied to the Golgi system. During secretion, this small fraction is added to the apical cell membrane, withdrawn by endocytosis, and at least partly broken down in lysosomes (9, 16). The other 99% of the membrane would then become superfluous in the Golgi system. According to this calculation, the genesis of one secretory granule requires at the level of the peripheral elements an amount of membrane equal to 100 times the granule membrane. Thus, per granule, (100 × $4\pi \cdot 0.6^2$ =) ~450 μm^2 membrane is added to the Golgi system. Such a quantum equals ~3% of the total amount of membrane present in the RER of a cell (in the guinea pig ~5% [3]). Lytic degradation of such amounts of membrane is unlikely and is inconsistent with the relatively long lifetimes of RER membrane constituents (21, 39). A return of superfluous Golgi membrane to the RER seems

FIGURE 13 Golgi system of an exocrine cell after feeding. Peripheral elements (*p*) and transitional elements of the RER (*tr*) are distributed along the outer side of the stacks of cisternae (*c*). At some places the meshworklike outermost Golgi cisternae (see also Fig. 9) can be recognized (between single arrowheads). The inner cisternae have strongly dilated parts and contain some flocculent material. At the inner side of the stacks, many condensing vacuoles (*cv*) of different sizes occur and most of them are completely filled with flocculent material. Structures typical for the Golgi centre, such as lamellae and coated vesicles, occur between the condensing vacuoles. (*n*), Nucleus, with polysome figures at its surface (double arrowheads). Bar, 1 μm. × 27,000.

FIGURE 14 Lumen in tissue after feeding. One secretory granule is fixed just at the moment of exocytosis (asterisks). Bar, 1 μm. × 15,000.

FIGURE 15 Basal part of an exocrine cell 2 h after feeding. Mitochondria encircling lipid droplets (*lip*), as depicted here, were commonly seen at that time. Bar, 1 μm. × 17,500.

therefore more likely. A possible membrane recycling at the level of the peripheral elements has already been mentioned by Jamieson and Palade (14). The idea of a shuttle movement of the small vesicles between RER and Golgi system seems compatible with some observations in the frog exocrine pancreas, suggesting that the peripheral elements represent a distinct class of membranous structures in the cell. First, these elements persist after fasting in spite of a strongly decreased amount of proteins that pass from the RER to the Golgi system. Similar observations are made in the mammalian pancreas under conditions of inhibited protein synthesis (20, 23). Second, the peripheral elements are specifically stained after osmium impregnation. Although little is known about the nature of this reaction, its occurrence in various cell types with presumably different contents of the elements (7) indicates that osmium blackening of the peripheral elements is caused by specific membrane properties rather than by the contents of the structure.

In the steady-state exocrine pancreatic cell of fasted mammals, where protein synthesis continues (24, 31), the formation of secretory granules is counterbalanced by a proportional "resting" secretion (19). In the frog pancreas, such an overflow secretion during fasting is probably less important because of the very low rate of protein synthesis. This consideration and the presence of a considerable amount of secretory granules after fasting indicate that, in the frog exocrine pancreas, secretion can be stopped very efficiently.

Received for publication 13 April 1978, and in revised form 14 November 1978.

REFERENCES

1. Amsterdam, A., and J. D. Jamieson. 1974. Studies on dispersed pancreatic exocrine cells. II. Functional characteristics of separated cells. *J. Cell Biol.* **63**:1057–1073.
2. Bedi, K. S., G. H. Cope, and M. A. Williams. 1974. An electron microscopic-stereologic analysis of the zymogen granule content of the parotid glands of starved rabbit and of changes induced by feeding. *Arch. Oral Biol.* **19**:1127–1133.
3. Bolender, R. P. 1974. Stereological analysis of the Guinea pig pancreas. I. Analytical model and quantitative description of nonstimulated pancreatic exocrine cells. *J. Cell Biol.* **61**:269–287.
4. Burri, P. H., H. Giger, H. R. Gnägi, and E. R. Weibel. 1968. Application of stereological methods to cytophysiologic experiments on polarized cells. *In* Electron Microscopy, Vol. 1. D. S. Bocciarelli, editor. IV European Conference, Rome. Tipografia Poliglotta Vaticana, Rome. 593–594.
5. Cope, G. H., and M. A. Williams. 1973. Quantitative analysis of the constituent membranes of parotid acinar cells and the changes evident after induced degranulation. *Z. Zellforsch. Mikrosk. Anat.* **145**:311–330.
6. Danielsson, Å., S. Marklund, and T. Stigbrand. 1974. Effects of starvation and islets hormones on the synthesis of amylase in isolated exocrine pancreas of the mouse. *Acta Hepato-Gastroenterol.* **21**:289–299.
7. Friend, D. S., and M. J. Murray. 1965. Osmium impregnation of the Golgi apparatus. *Am. J. Anat.* **117**:135–150.
8. Fujita, H. 1975. Fine structure of the thyroid gland. *Int. Rev. Cytol.* **40**:197–280.
9. Geuze, J. J., and M. F. Kramer. 1974. Function of coated membranes and multivesicular bodies during membrane regulation in stimulated exocrine pancreas cells. *Cell Tiss. Res.* **156**:1–20.
10. Geuze, J. J., and C. Poort. 1973. Cell membrane resorption in the rat exocrine pancreas cell after in vivo stimulation of the secretion, as studied by in vitro incubation with extracellular space markers. *J. Cell Biol.* **57**:159–174.
11. Giger, H., and H. Riedwyl. 1970. Bestimmung der groszenverteilung von kugeln aus schnittkreisradien. *Biom. Z.* **12**:156–162.
12. Hand, A. R., and C. Oliver. 1977. Cytochemical studies of GERL and its role in secretory granule formation in exocrine cells. *Histochem. J.* **9**:375–392.
13. Hokin, L. E. 1968. Dynamic aspects of phospholipids during protein secretion. *Int. Rev. Cytol.* **23**:187–208.
14. Jamieson, J. D., and G. E. Palade. 1967. Intracellular transport of secretory proteins in the pancreatic exocrine cell. I. Role of the peripheral elements of the Golgi complex. *J. Cell Biol.* **34**:577–596.
15. Jamieson, J. D., and G. E. Palade. 1971. Synthesis, intracellular transport, and discharge of secretory proteins in stimulated pancreatic exocrine cells. *J. Cell Biol.* **50**:135–158.
16. Kalina, M., and R. Robinovitch. 1975. Exocytosis couples to endocytosis of ferritin in parotid acinar cells from isoprenalin stimulated rats. *Cell Tiss. Res.* **163**:272–283.
17. Kohler, P. O., P. M. Grimley, and B. W. O'Malley. 1969. Estrogen-induced cytodifferentiation of the ovalbumin-secreting glands of the chick oviduct. *J. Cell Biol.* **40**:8–27.
18. Kramer, M. F., and C. Poort. 1968. Protein synthesis in the pancreas of the rat after stimulation of secretion. *Z. Zellforsch. Mikrosk. Anat.* **86**:475–486.
19. Kramer, M. F., and C. Poort. 1972. Unstimulated secretion of protein from rat exocrine pancreas cells. *J. Cell Biol.* **52**:147–158.
20. Longnecker, D. S., H. Shinozuka, and E. Farber. 1968. Molecular pathology of in vivo inhibition of protein synthesis. Electron microscopy of rat pancreatic acinar cells in puromycin-induced necrosis. *Am. J. Pathol.* **52**:891–915.
21. Meldolesi, J. 1974. Dynamics of cytoplasmic membranes in Guinea pig pancreatic acinar cells. I. Synthesis and turnover of membrane proteins. *J. Cell Biol.* **61**:1–13.
22. Meldolesi, J., P. De Camilli, and D. Peluchetti. 1975. The membrane of secretory granules: Structure, composition and turnover. *In* Secretory Mechanisms of Exocrine Glands. N. A. Thorn and O. H. Petersen, editors. Academic Press, Inc., New York. 137–148.
23. Melmed, R. N., C. J. Benitez, and S. J. Holt. 1973. An ultrastructural study of the pancreatic acinar cell in mitosis with special reference to changes in the Golgi complex. *J. Cell Sci.* **12**:163–173.
24. Morisset, J. A., and P. D. Webster. 1972. Effects of fasting and feeding on protein synthesis by the rat pancreas. *J. Clin. Invest.* **51**:1–8.
25. Nevalainen, T. J., and D. T. Janigan. 1974. Degeneration of mouse pancreatic acinar cells during fasting. *Virchows Arch. Abt. B Zellpathol.* **15**:107–118.
26. Novikoff, A. B., M. Mori, N. Quintana, and A. Yam. 1977. Studies of the secretory process in the mammalian exocrine pancreas. I. The condensing vacuoles. *J. Cell Biol.* **75**:148–165.
27. Orci, L., A. Perrelet, and A. A. Like. 1972. Fenestrae in the rough endoplasmic reticulum of the exocrine pancreatic cells. *J. Cell Biol.* **55**: 245–249.
28. Oron, U., and A. Bidolah. 1973. Regulation of protein synthesis in the venom gland of viperid snakes. *J. Cell Biol.* **56**:177–190.
29. Palade, G. E., P. Siekevitz, and L. G. Caro. 1962. Structure, chemistry and function of the pancreatic exocrine cell. *In* The exocrine pancreas. A. V. S. de Reuck and M. P. Cameron, editors. Churchill (J. & A.) Ltd., London. 23–48.
30. Pantic, V. R. 1975. The specificity of pituitary cells and regulation of their activities. *Int. Rev. Cytol.* **40**:153–195.
31. Poort, C., and M. F. Kramer. 1969. Effects of feeding on the protein synthesis in mammalian pancreas. *Gastroenterology.* **57**:689–696.
32. Redman, C. M., P. Siekevitz, and G. E. Palade. 1966. Synthesis and transfer of amylase in pigeon pancreatic microsomes. *J. Biol. Chem.* **241**:1150–1158.
33. Regard, E., and J. Hourdry. 1975. Modifications structurales des cellules thyroidiennes chez la larve du xénope traitée par la prolactine ovine. Incidences sur le métabolisme de l'iode. *J. Microsc. Biol. Cell.* **22**:39–54.
34. Slot, J. W., J. J. Geuze, and C. Poort. 1974. Synthesis and intracellular transport of protein in the exocrine pancreas of the frog (*Rana esculenta*). I. An ultrastructural and autoradiographic study. *Cell Tiss. Res.* **155**:135–154.
35. Slot, J. W., J. J. Geuze, and C. Poort. 1976. Synthesis and

intracellular transport of proteins in the exocrine pancreas of the frog (Rana esculenta). II. An in vitro study of the transport process and the influence of temperature. *Cell Tiss. Res.* **167:**147–165.

36. SLOT, J. W., G. J. A. M. STROUS, and J. J. GEUZE. 1979. The effect of fasting and feeding on synthesis and intracellular transport of proteins in the frog exocrine pancreas. *J. Cell Biol.* **80:**708–714.
37. SPARROW, A. H., H. J. PRICE, and A. G. UNDERBRINK. 1972. A survey of DNA content per cell and per chromosome of prokaryotic and eukaryotic organisms: Some evolutionary considerations. *In* Evolution of Genetic Systems. H. H. Smith, editor. Gordon and Breach, Science Publishers, Inc., New York. 451–494.
38. VAN VENROOIJ, W. J., and C. POORT. 1971. Rate of protein synthesis and polyribosome formation in the frog pancreas after fasting and feeding. *Biochim. Biophys. Acta.* **247:**468–470.
39. WALLACH, D., N. KIRSHNER, and M. SCHRAMM. 1975. Nonparallel transport of membrane proteins and content proteins during assembly of the secretory granule in rat parotid gland. *Biochim. Biophys. Acta.* **375:**87–105.
40. WEIBEL, E. R., and R. P. BOLENDER. 1973. Steriological techniques for electron microscopic morphometry. *In* Principles and Techniques of Electron Microscopy, Vol. 3. M. A. Hayat, editor. Van Nostrand Reinhold Company, New York. 237–296.